Bulletin of Earthquake Engineering
https://doi.org/10.1007/s10518-023-01673-3

S.I. : GEOTECHNICAL SEISMIC ISOLATION

Rubber-soil mixtures: use of grading entropy theory to evaluate stiffness and liquefaction susceptibility

Juan Bernal-Sanchez[1] · **James Leak**[1] · **Daniel Barreto**[1]

Received: 4 July 2022 / Accepted: 16 March 2023

Abstract
Rubber-soil mixtures are known to have mechanical properties that enable their use in backfills, road construction or geotechnical seismic isolation systems. The complexity of these mixtures comes from adding soft (i.e. rubber) particles that increases the number of particle properties to consider when studying the macroscopic behaviour. The distinction between sand-like and rubber-like behaviour is normally presented in relation to the rubber content and size ratio between particles. It is however unknown how the change on the mixture gradation affects the mechanical behaviour of RSm. Entropy coordinates condense the entire particle size distribution (PSD) to a single point on a Cartesian plane, accounting for all the information in the gradation. Grading entropy coordinates have been used to study typical geotechnical behaviours of mostly incompressible (i.e. sand) soils. In this study, entropy coordinates are used to analyse the correlation between the small-strain stiffness and liquefaction susceptibility of RSm and their PSDs. The results suggest that entropy coordinates can be used effectively on RSm as an alternative means of assessment of typical soil behaviours, being also able to distinguish between sand-like and rubber-like behaviours. Based on the 30 PSDs analysed, it is also evidenced that internal stability criterion proposed by Lőrincz (1986) can be used to predict the liquefaction susceptibility of RSm. The normalised base entropy (A) has also been shown to increase with the rubber content, which is linked to a lower liquefaction susceptibility, due to the supporting effect of rubber particles on strong-force chains formed of sand particles.

Keywords Rubber-soil mixtures · Grading entropy coordinates · Internal stability · Liquefaction susceptibility · Force transmission

List of symbols

ΔS Entropy increment
S_0 Base entropy
A Normalised base entropy increment
B Normalised entropy increment

✉ Juan Bernal-Sanchez
J.Bernal-Sanchez@napier.ac.uk

[1] School of Engineering and the Built Environment, Edinburgh Napier University, Merchiston Campus, Edinburgh EH10 5DT, UK

Published online: 02 April 2023

1 Introduction

Civil engineering projects are often large scale, time sensitive, and crucially: material intensive. There is also, undoubtedly, a global waste problem. As such, great effort has been made to incorporate recycled material into engineering projects (European Communities 2006). One of the most abundant waste materials available are scrap tyres. The disposal of scrap tyres has become a major environmental problem in many countries around the world. The high durability in addition to the strength of the vulcanised rubber has made the recovery of the material difficult, hence used tyres typically end up in landfills or stockpiles (ETRMA 2015). Tyres have however a number of opportunities for repurpose in Civil Engineering infrastructure, including the production of cement mixtures, road construction and geotextiles (Xiong and Li 2013). One of the more interesting applications is the combination of rubber-sand mixtures (RSm) and its ability to be used as a Geotechnical Seismic Isolation (GSI) technology to offset the destructive effects of seismic events (Tsang et al. 2012). However, the use of RSm is still relatively new, and in this regard, its use in permanent (long-term) constructions is still questioned. Moreover, the range of tyre aggregates is large, affecting the properties of RSm such as stiffness, particle size, shape, and overall content (e.g., Kim and Santamarina 2008; Anastasiadis et al. 2012; Senetakis et al. 2012).

1.1 Rubber-soil mixtures

The complexity of understanding the response of Rubber-Sand mixtures (RSm) under loading stems from adding "soft" particulate rubber to a material originally consisting of rigid particles. The binary skeleton of RSm is a combination of rigid-soft particles which interact at a particulate level and may influence the macroscopic behaviour depending on aspects such as the rubber content or size ratio between sand and rubber particles (Kim and Santamarina 2008).

A broad view of how RSm behaves in comparison with a conventional (incompressible) soil points unambiguously to an increase in compressibility (Masad et al. 1996; Youwai and Bergado 2003). With regards to the strength, the picture is less clear: considering only the static case, shearing resistance may increase or decrease due to the addition of rubber (Sheikh et al. 2012). This entails the study of additional particle properties such as rubber mass, size, shape, or stiffness and its interaction with sand particles. The dominant behaviour of RSm is however not only dictated by the particle properties but also the test conditions, i.e. mean stress (Anastasiadis et al. 2012; Senetakis et al. 2012). The existence of such a vast number of factors leads to a scenario where the evaluation of both static and dynamic behaviour is challenging.

For example, Zornberg et al., (2004) noted that mixtures of rubber (big) chips below 35%-40% exhibit high shear strength and appropriate compaction characteristics. The static behaviour changed above 35% rubber exhibiting a fully contractive behaviour and a reduction in friction angle. Lee et al. (2010) postulated that load carrying force chains were created along the stiff sand skeleton, whilst the addition of rubber resulted in a reduction of the peak strength. The concepts of sand-like behaviour; characterised for exhibiting higher small-to-large stiffness, and rubber-like behaviour; defined as a mixture that presents lower shear moduli and deforms more easily under loading, were thus

consolidated to explain the evolution in the macro-scale parameters of RSm (Lee et al. 2007; Kim and Santamarina 2008).

Another property considered in the literature has been the rubber shape. Edincliler et al. (2010) demonstrated that an increase in the aspect ratio of rubber fibres enhances the shear strength by adding rubber content above 20%. Fu et al. (2017) showed how tyre crumbs do not contribute to the rise in the peak shear strength and only 30% of rubber fibres can lead to higher values, which was attributed to the reinforcing effect of elongated particles. Thus, rubber-like behaviour is more prominent with the addition of rubber crumbs. According to Sheikh et al. (2012) and Fu et al. (2017), this can be reverted, and the sand-like behaviour be more apparent when altering rubber size either by increasing its length, i.e. aspect ratio, or with bigger rubber particles.

Regarding the dynamic behaviour of RSm, this has been widely studied for its potential application when used in a GSI system (Tsang 2009; Tsang and Pitilakis 2019). For that, the shear modulus and damping ratio, which characterise the soil dynamic properties, have to be understood at very small strains. Previous studies (Anastasiadis et al. 2012; Mashiri et al. 2016; Bernal-Sanchez et al. 2019, 2020) gathered experimental results showing the change in dynamic behaviour of RSm. The literature coincides that the small strain shear stiffness of RSm increases with confining pressure, but it decreases with rubber content and shear strain amplitude. This reduction in stiffness appeared however more attenuated during the sand-like behaviour, at rubber contents below 35% and when increasing the size ratio. However, even with the extended experimental data on static and dynamic behaviour, no correlation has been established yet between the change in stiffness of RSm and the particle (size) gradation of the mixture.

It should be noted that the previously mentioned shift in mechanical behaviour is not entirely unique to RSm. It is well understood that with the addition of fines to soils, there exists a point in which the mechanical response shifts from sand-dominated to fine-dominated. The is distinguished by a fines content (FC) threshold, commonly reported at around 30–40% FC (Thevanayagam 1998). The concept of the threshold fines concept is useful as it relates to the concept of skeletal void ratio. In other words, it helps to differentiate state conditions in which coarse particles float on a matrix of finer particles, or those in which finer particles simply fill the inter-particle voids of coarse grains and provide no load-carrying capacity to the soil skeleton.

Additional similarities in behaviour can be created between the addition of rubber particle and the inclusion of FC in a soil. According to the literature, the effect of adding FC to a soil leads to increasing its liquefaction resistance (Okashi 1970), or, on the other hand, inhibits the stability of the grains, leading to a greater liquefaction susceptibility (Baziar and Dobry 1995). But, as addressed in the literature, the effect of FC on the undrained response of a soil is not only attributed to the amount of fines. Moreover, the choice in state measure (i.e., relative density or void ratio) chosen either pre or post consolidation is an important factor (Ress 2010; Gobbi et al. 2021). Also, the addition of plastic fines has been suggested to increase the liquefaction resistance of soils due to the increase in the cohesive strength (Guo and Prakash 1999; Perlea 2000; Tsai et al. 2019).

With regards to the liquefaction susceptibility of RSm, existing research has demonstrated that introducing tyre derived aggregates (Kaneko et al. 2013; Mashiri et al. 2016), particulate rubber (Otsubo et al. 2016; Bernal-Sanchez et al. 2020) or tyre powder (Bahadori and Roohollah 2018) leads to a significant reduction in the accumulation of pore water pressure. The latter would result in an improvement of the liquefaction resistance and a higher stability against cyclic loading of sand specimens. Most of these studies point to the deformability of rubber to account for the higher liquefaction resistance. On

the other hand, Promputthangkoon and Hyde (2008), testing mixtures with tyre chips, and Shariatmadari et al. (2018), with granulated rubber, found that liquefaction resistance of RSm decreases by adding rubber. Despite the current knowledge, no previous study has attempted to study the dependency between the RSm gradation (i.e. PSD) and their liquefaction susceptibility.

Commonly used gradation-based methods are used to assess the liquefaction susceptibility of a soil. This is the case for classifications that consider particle descriptors such as the mean particle size (d_{50}) and the coefficient of uniformity (C_u) (Isihara 1997). The proposed limits proposed by Tokimatsu and Yoshimi (1983) are still being used today to assess the liquefaction susceptibility of soils dividing them into well-graded and poorly-graded soils. Despite the extensive empirical data, the latter approach (Tokimatsu and Yoshimi 1983) appears to be problematic for certain soils. A possible reason for this is that PSD descriptors used only account for individual particle diameters (e.g. d_{50} and $c_u = d_{60}/d_{10}$). Such parameters clearly ignore the content of fines and gravels in soils. An alternative approach should thus be used to consider the whole PSD of the soil.

Grading entropy is a method that uses principles akin to information entropy. It has been adopted to effectively explain the relationship between the gradation and geotechnical phenomena such as particle breakage evolution (Lőrincz 2005; Leak et al. 2021), the dependence of small strain shear stiffness on gradation (Barreto and Imre 2018) and liquefaction susceptibility (Barreto et al. 2019), amongst others. The addition of rubber into sand raises interesting questions, particularly in regard to the soils stiffness and overall strength. How much does rubber contribute to stress transmission? How significant is the importance of changes in void ratio as rubber is added? How are these things influenced by the rubber flexibility and other characteristics? What is the effect of the PSD of the RSm on its mechanical behaviour? In this study, a simple and effective criterion that may be used to assess the susceptibility to liquefaction of RSm using grading entropy coordinates is proposed for the first time. The results also provide a clear link between the gradation of RSm and its shear stiffness that extend our understanding beyond the dependence of stiffness on just rubber content, size ratio between rubber and sand particles or rubber shape.

1.2 Mechanical behaviour of RSm

The mechanical behaviour of RSm has been extensively characterised in the literature. On the basis of resonant column and cyclic triaxial tests (Bernal-Sanchez et al. 2018, 2019, 2020), a reduction in soil shear stiffness, both with shear strain and rubber content has been addressed (Fig. 1a). The latter is explainable by the presence of deformable rubber particles. Stiffness decays for all rubber percentages when applying larger strain amplitudes. This phenomenon is observed to be more pronounced at low rubber percentages (e.g. 0–10% by mass), as one would expect for a pure sand and RSm in which the sand fraction is dominant, i.e. sand-like behaviour (Lee et al. 2010). On the other hand, the initial stiffness and subsequent decrease with strain amplitude is lower in specimens containing higher rubber contents (e.g. 20–30% by mass), i.e. rubber-like behaviour (Kim and Santamarina 2008), and it implies a greater ability to withstand large deformations.

With regards to the damping capacity of RSm, it is proven that energy dissipation occurs due to the development of friction between sliding sand particles (Senetakis et al. 2012) in addition to the deformation experienced by rubber particles (Fonseca et al. 2019). Experimental results (Fig. 1b) show that, in general terms, adding particulate rubber to sand leads

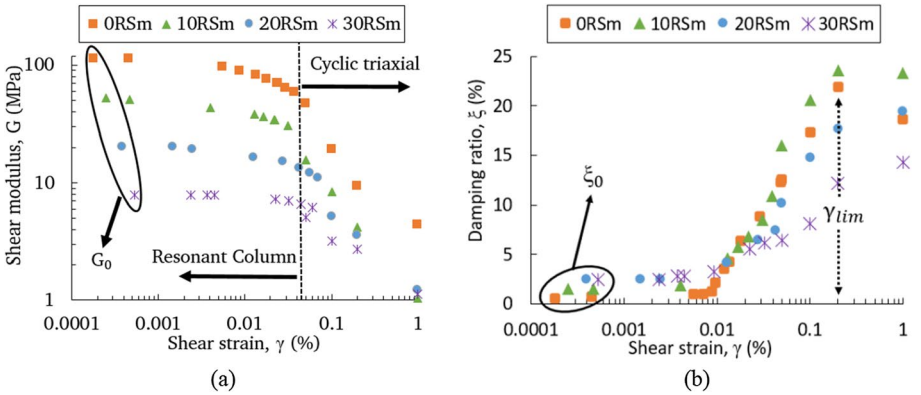

Fig. 1 **a** Shear modulus and **b** damping ratio of RSm from small-to-large strains (Bernal-Sanchez 2020)

to an improvement of both the viscous (small strain) damping and hysteretic (large strain) damping.

2 Grading entropy

Proposed by Lőrincz (1986), grading entropy coordinates have been used to further understand the evolution of particle breakage (Leak et al. 2022), the prediction of permeability (O'Kelly and Nogal 2020; Feng et al. 2019). Oquendo and Estrada (2022) also applied grading entropy coordinates to particle jamming, revisiting the Fuller and Thompson distribution. Grading entropy coordinates enable the entirety of a soil PSD to be assessed. This is achieved via summation of the entropy in each individual fraction (i.e. mass percentage retained in each sieve), allowing the total entropy (Eq. 1) of the distribution to be represented by a single point on a cartesian plane:

$$S = \Delta S + S_0 \tag{1}$$

where S is the total grading entropy, ΔS is the entropy increment, and S_0 is the base entropy. ΔS and S_0 are the (non-normalised) grading entropy coordinates and make the coordinate pair that may represent any PSD. The entropy increment (ΔS), normally plotted on the y-axis, is defined as:

$$\Delta S = -\frac{1}{\ln(2)} \sum_{i=1}^{n} x_i ln x_i \tag{2}$$

where n is the number of the fractions (i.e. sieves) between the finest and coarsest particles, x_i is the relative frequency of the fractions (i.e. mass percentage retained) and the base entropy (S_0), normally plotted on the x-axis, is given by:

$$S_0 = \sum_{i=1}^{n} x_i S_{oi} \tag{3}$$

Table 1 The intrinsic entropy (S_0) corresponding to their soil fractions (Barreto et al. 2019)

Fraction	0	…	22	23	24
d (mm)	$2^{-22}2^{-21}$		1–2	2–4	4–8
S_o (−)	0		22	23	24

In Eq. (3), S_{oi} is the intrinsic entropy, an integer which increases relative to standard sieve sizes, as seen in Table 1.

These coordinates have simple physical meanings. The base entropy (S_0) is a logarithmic mean of the average grain diameter and relates to the skewness of the PSD. The entropy increment (ΔS) is a measure of how much a soil is influenced by its fractions and it relates to the kurtosis of the distribution. While S_0 may be related to d_{50} and ΔS to the coefficient of uniformity (C_u), it must be noted that the entire PSD is considered by these coordinates.

Note that ΔS and S_0 have normalised variants, where $0 < A < 1$ and $0 < B < B_{max} \cong 1.41$. Here, 'A' is the normalised base entropy and 'B' is the normalised entropy increment, given by:

$$A = \frac{S_0 - S_{0min}}{S_{0max} - S_{0min}} \tag{4}$$

$$B = \frac{\Delta S}{\ln(N)} \tag{5}$$

PSDs which are uniformly sized (narrow range of particle diameters) have a low entropy increment, whilst those PSDs representing well-graded specimens will have large values of the entropy increment (ΔS and B).

2.1 Grading entropy of RSm

Figure 2 represents the grading entropy coordinates of RSm at different rubber contents based on the oedometer (with bender elements) results obtained by Lee et al. (2010). The

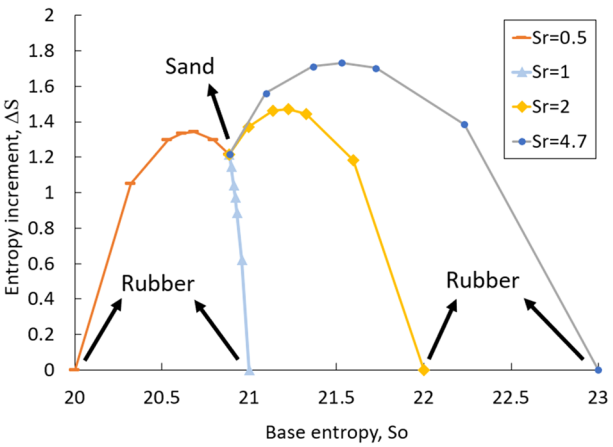

Fig. 2 Grading entropy of RSm with change in size ratio based on Lee et al. (2010)

latter established that constrained modulus and small strain shear modulus decrease with the inclusion of rubber or decrease in sand fraction at any size ratio. This was explained on the basis that the mixture stiffness is controlled by load chains created along the sand skeleton. The results from these experiments have been used in this and the following sections due to the high variety of material characteristics, and varying size ratio (i.e. ratio between rubber and sand particles), associated with RSm.

For clarity and completeness, Lee et al. (2010) used Jumunjin 20/30 sand which is a coarse, uniform, and angular sand with the following physical properties: $e_{min}=0.60$, $e_{max}=0.87$, $D_{50}=0.725$ mm, specific gravity = 2.62, roundness = 0.7–0.9, sphericity = 0.9, Poisson's ratio = 0.3, shear modulus = 100 MPa. In the RSm, shredded tires had the following properties: specific gravity = 1.15–1.17, roundness = 0.1–0.5, sphericity = 0.5–0.9, Poisson's ratio = 0.49, and shear modulus = 1 MPa. Six uniform sizes of shredded rubber were used with $D_{50}=3.375$, 1.425, 0.725, 0.513, 0.363, 0.256 mm.

Equations 2 and 3 have been adopted to determine the entropy increment and base entropy of the RSm, respectively. The results presented in Fig. 2 correspond to four (out of six) size ratios (S_r) analysed in this study, in which the sand size is maintained, and the rubber size changes: $S_r=4.7$ (highest rubber size), 2, 1 and 0.5 (smallest rubber size). Also note that grading entropy coordinates as illustrated here considered the PSD of the RSm in full (i.e. without considering rubber/sand separately, the equivalent of sieving a sample of the corresponding mix).

The point where all lines converge is as expected, the point that represents the PSD of the host sand. The addition of rubber to sand leads to a change in the PSD of the mixture, hence a change of grading entropy coordinates. Entropy coordinates change as the rubber content (in terms of volume) increases, $V_{rubber}/V_{total}=0$, 0.2, 0.4, 0.5, 0.6, 0.8 and 1. In the end, they diverge to four different points which correspond to mixtures with 100% rubber but different (rubber) sizes. Also note that the point of maximum curvature for each S_r represents the "most well-graded" of mixes. In other words, the mix with most size fractions, or material retained in the largest number of sieves. The highest values of the entropy increment are found at 40% and 50% rubber contents. Note the similarity of values with the threshold fines content discussed before.

The reason why the four size ratios are associated with a final null entropy increment (i.e. $\Delta S=0$) is because all rubber particles added to sand in the mixtures have uniform size and no other size fractions exist (i.e. all material can be gathered in a single sieve).

As previously described, the base entropy (S_0) is related to the average grain diameter of the soil. Therefore, the base entropy decreases with the rubber content if the particles added are of smaller size, as observed in $S_r=0.5$, and it increases if the rubber particles are of bigger size ($S_r=2$ and 4.7). Following this approach, the base entropy should remain the same at $S_r=1$. The slight deviation from the vertical on Fig. 2 may be explained by small quantities of non-uniform particle sizes retained on a limited number of sieves. At a larger scale, Fig. 2 shows how the addition of larger rubber particles ($S_r=4.7$) leads to PSDs with higher ΔS. The same occurs with the S_0.

3 Grading entropy & stiffness

Barreto and Imre (2018) undertook a direct comparison of grading entropy coordinates and descriptors such as coefficient of uniformity (C_u) and new PSD parameter (C_g) used to quantify small strain shear stiffness. Using experimental data from Wichtmann and

Triantafyllidis (2009) the normalised entropy coordinates (A & B) where shown to be highly sensitive to quantifying shear stiffness. Moreover, a unique linear relationship was found between the grading entropy coordinates and the small strain shear stiffness. In their data, B does not significantly affect the soils stiffness. However, it was able to discriminate the stiffness' dependence on stress level, supporting the idea of larger stresses engaging a larger number of contacts and hence a larger stiffness. Within this context, B relates to the stress distribution via the mobilisation of force chains and may indicate that for the same PSD a larger number of particles are required to transmit/sustain a higher stress level, or alternatively, depending on the PSD, more particle sizes may be required to sustain higher stresses.

In the same study, Barreto and Imre (2018) argued that 'A' is a much more effective parameter to estimate the stiffness than other existing relationships as a function of d_{50} and c_u. They also explained the relationship between 'A', the stiffness and stress transmission by postulating that well graded samples may have significantly larger number of contacts than those that are uniformly graded. It must however be noted that stiffness may also be affected by particle shape (for example, due to presence of particles contacting over large/small areas) and mineralogy (i.e. quartz/carbonate sands or relevant to this study, rubber properties).

3.1 Small-strain stiffness of RSm

In order to assess the effectiveness of the grading entropy coordinates to estimate the dependency between grading of RSm and their small strain shear stiffness, the results by Lee et al. (2010) were re-examined. Figure 3 illustrates a comparison between shear modulus and base entropy (S_0) at various size ratios and at a confining pressure of 320 kPa. Note that the use of high confining pressures is justified if deep mitigation procedures are proposed. For example, Mahdavisefat et al. (2017) suggested the use of RSm deep filled trenches, Tsang et al. (2021) considered 3 m depth, and Bernal-Sanchez et al. (2022) discussed the possible use of bagged RSm vertical installations adjacent to structures that could be excavated at depths of up to 30 m with standard piling equipment.

In line with previous studies (Senetakis et al. 2012; Bernal-Sanchez et al. 2018, 2019), the shear stiffness decreases with the addition of rubber as a result of the capacity to deform of rubber particles. However, different trends are observed depending on

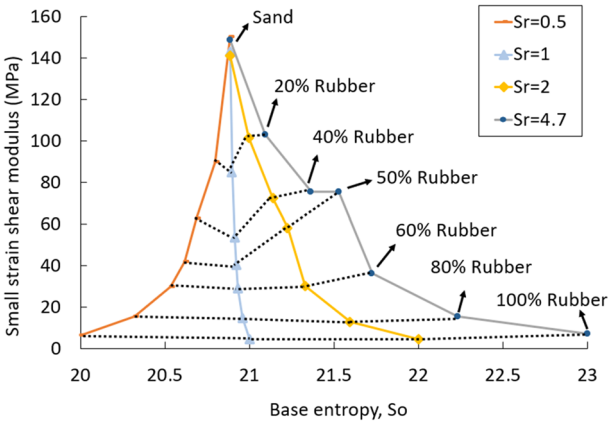

Fig. 3 Change in soil stiffness of RSm with base entropy (S_0) and size ratio at 320 kPa of confining pressure based on Lee et al. (2010)

the size ratio between rubber and sand particles. The addition of bigger rubber particles leads to higher values of S_0, which also results in a reduction of the mixture stiffness. The latter is (possibly) a consequence of having force chains created amongst the big rubber particles which deform and are not able to resist large stresses, resulting in a lower shear stiffness. The same trend is observed in this study for mixtures with bigger sand particles ($S_r = 0.5$). In this case, although force chains are created amongst the bigger sand particles, the smaller rubber particles are unable to (laterally) support these force chains, which then may buckle and collapse, producing the observed stiffness reduction. Notably however, Fig. 3 demonstrates that entropy coordinates are useful to explain the dependence of stiffness in terms of both size ratios, particle size distribution and rubber content.

Furthermore, Fig. 3 also provides an alternative interpretation of the sand-like, and rubber-like and transitional behaviour in line with Lee et al. (2010). As observed in Fig. 3, the shear modulus of RSm is low at high rubber contents (60%, 80% and 100% rubber), which represents a typical rubber-like behaviour, and it remains relatively similar with different size ratios (i.e. dotted lines joining equal rubber content and different S_r remain predominantly horizontal). As the rubber content decreases, the increase in stiffness is more noticeable with bigger rubber particles ($S_r = 4.7$, $S_r = 2$) as compared to mixtures with similar size ratio ($S_r = 1$). Note that the dotted lines are now more curved. This is in line with findings from Anastasiadis et al. (2012) and Kim and Santamarina (2008), who showed how the sand-like behaviour is more prominent at rubber contents < 35% and higher size attributed to an increase in the sand-to-sand contacts and hence the control of the behaviour by the soil (incompressible) matrix.

Although it is difficult to set where the transitional behaviour takes place, it is however observed that the size ratio of RSm influences the stiffness degradation, and this is more evident at 20% to 50% rubber contents. More data may be able to relate this transition to the same physical phenomena explaining the threshold fines content effect, but this is not within the scope of this investigation.

Figure 4 illustrates the change in shear stiffness and entropy increment with the size ratios at 320 kPa of confining pressure. A relationship is again found between the mixture grading and its stiffness. At similar size ratio ($S_r = 1$), the stiffness decreases with the reduction in the entropy increment. The latter suggests that for a certain stress level,

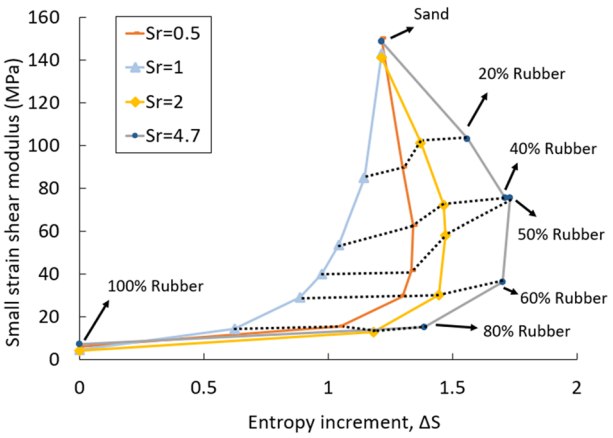

Fig. 4 Change in soil stiffness of RSm with entropy increment (ΔS) and size ratio at 320 kPa of confining pressure based on Lee et al. (2010)

the shear stiffness is only dependant on the rubber content and the range of particle sizes retained in (limited) sieves.

A reduction in the mixture stiffness also occurs at other size ratios ($S_r = 0.5$, 2, 4.7). However, in these cases there is an increase in ΔS followed by slight decrease as the rubber content decreases. Interestingly, the pattern of near horizontal contour lines of equal rubber content is also observed to identify rubber-like behaviour and curved contour lines for sand-like behaviour as discussed with reference to S_0. The dependence of shear stiffness on rubber content and size ratio is also clear here.

Recall that ΔS measures how much of the soil behaviour is influenced by all the fractions. In other words, how many fractions (sieves) are represented within the mixtures. Consequently, a higher value of ΔS may describe a higher number of inter-particle contacts (because mixtures are better graded). This would also support the hypothesis of the development of primary load-carrying chains created between sand-to-sand contacts either after the distortion of rubber particles ($S_r = 0.5$) or before the rubber deforms ($S_r = 2$, 4.7).

The dependency between stiffness and grading of RSm has been illustrated in Fig. 5 at various stress levels. On this occasion, mixtures with three size ratios have been considered for comparison: $S_r = 0.5$, 1 and 2. First, as expected, stiffness always increases with stress level. It can be also observed that whether the stiffness reduces or increases with an increase in S_0 for a given stress level is only dependent on size ratio. For $S_r < 1$ the stiffness increases with S_0 and for $S_r > 1$ it decreases with S_0. Note that for $S_r = 1$ the change in stiffness is nearly independent from S_0 and only affected by rubber content, as discussed before.

One advantage of presenting the results in this format is the ability to create contour zones of equal rubber content as illustrated in Figs. 3 and 4. Contour lines show the "summit" surrounding the specimens with equal size ratio. The shape of such contour lines may also be explained as follows. Sand-to-sand contacts develop higher stress transmission in mixtures with $S_r = 0.5$ before the distortion of rubber particles takes place at low stress levels. Note this happens under low percentage of rubber. However, as rubber content increases, the mixture with smaller sand particles ($S_r = 2$) may experience more sand-to-sand contacts, creating primary-load carrying forces across the matrix after the distortion of rubber, hence increasing stiffness.

The latter phenomenon is in line with the concept established by Lee et al. (2010) that the increase in stress level leads to greater inter-particle contacts, and that more primary

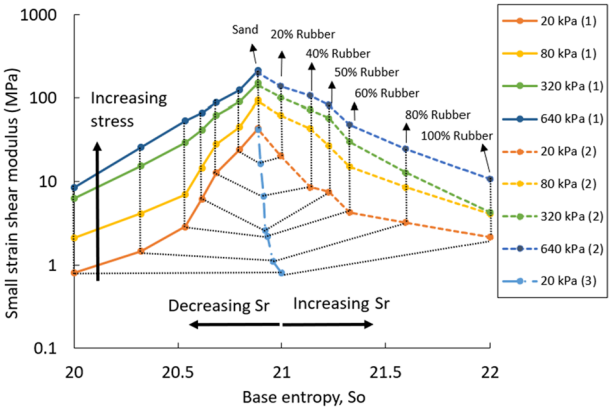

Fig. 5 Change in soil stiffness of RSm with base entropy (*So*) and confining pressure at $S_r = 0.5$ (1), $S_r = 2$ (2), and $S_r = 1$ (3) based on Lee et al. (2010)

load-carrying chains are created amongst the small sand particles. However, this phenomenon is less appreciable at very large stress levels (i.e. 320 kPa and 640 kPa) and mixtures with both size ratios ($S_r = 0.5$ and 2) show relatively similar shear stiffness. This is attributed to the idea that rubber particles fully distort at such a high stress level and the development of the strength in the mixtures is mainly a result of the sand-to-sand contacts.

Figure 6 illustrates the stiffness and entropy increment of RSm at various stress levels. Note that the trends at 320 kPa for both size ratios have already been illustrated in Fig. 4. As mentioned in Fig. 5, the application of greater stress levels results in a greater stiffness of the mixture at any size ratio. The evolution in ΔS is different depending on the size ratio of the mixture (Fig. 6). The mixtures containing similar particle sizes ($S_r = 1$) exhibit a gradual increase in the value of ΔS, which represents the number of fraction sizes acting in the mixture, with the reduction in the rubber content (Fig. 6a). Interestingly, the evolution of the trends shows how the mixtures start from a common point, a low stiffness associated with rubber only mixtures, and they diverge into four points that represent the greater stiffness of sand only samples. Thus, the highest value of ΔS coincides with the highest stiffness of RSm. With bigger rubber particles ($S_r = 4.7$), the evolution in ΔS follows a different trend as illustrated in Fig. 6b. The highest stiffness exhibited by the mixtures (i.e. sand only) does not align with the maximum value of ΔS. Regardless the stress level, it is observed that the maximum entropy increment occurs at 50% rubber volume. Whilst this may also relate to the transition between sand-like and rubber-like behaviour, it may also indicate the inefficient role of rubber particles to support strong force chains as rubber content increases.

4 Internal stability rule and its relationship with liquefaction phenomena

Lőrincz (1986) using suffusion test data, discussed an internal stability criterion using grading entropy coordinates (as defined in Sect. 2) which is explained here with reference to Fig. 7. The figure shows a partly non-normalised entropy diagram together with limiting lines as a function of the number of fractions N used to calculate such lines that

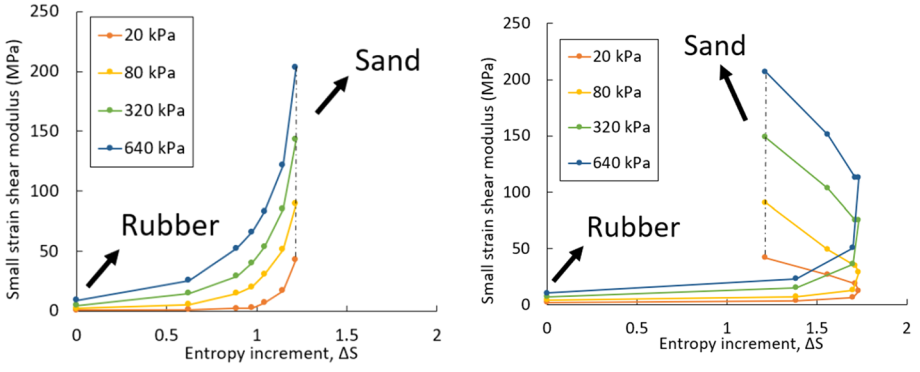

Fig. 6 Change in soil stiffness of RSm with entropy increment (ΔS) and confining pressure at a) $S_r = 1$ and b) $S_r = 4.7$ based on Lee et al. (2010)

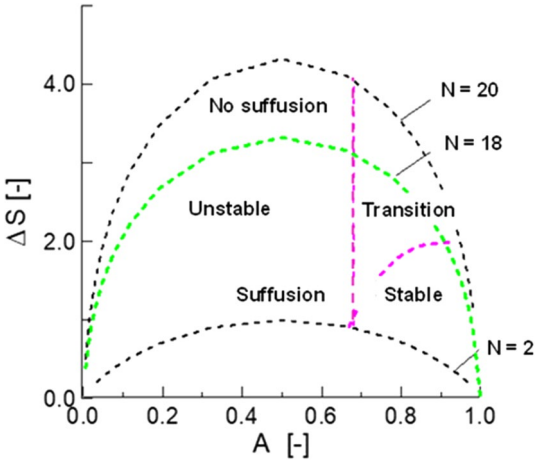

Fig. 7 Internal or grain structure stability criterion in the partly normalized diagram (modified after Lőrincz 1986)

illustrates three main zones: $A < 2/3$, where mixtures are internally unstable, $A = 2/3$ and $A > 2/3$ where soils are internally stable. Suffusion may occur in each zone if the geometric condition is met (i.e., gap-graded soils). The rule can be interpreted such that when $A > 2/3$, coarse particles may "float" in a matrix of fines and thus become destabilised if fines are removed (suffusion). Note that the occurrence of suffusion also depends on polydispersity (as indicated by the no suffusion zone when $N > 18$). In the transition zone, also denoted by points 'BCD' in Fig. 7, if $A = 2/3$ and $A > 2/3$, coarse particles form a skeleton and total erosion cannot occur and the structure of larger particles is inherently stable.

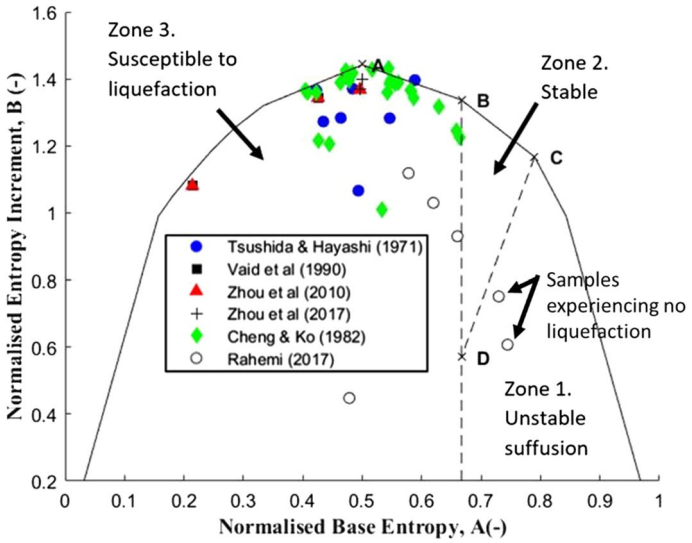

Fig. 8 PSDs representing liquefaction susceptibility limits, as discussed by Barreto et al. (2019). Points A, B, C & D on a normalised entropy diagram are used to demonstrate regions of soil internal stability phenomena as proposed by Lőrincz (1986)

In an attempt to link the internal stability criterion to liquefaction, Barreto et al. (2019) analysed 39 PSDs form different sources (data including experiments, field data and DEM simulations) which were known to liquefy (Fig. 8). Notably, the data included in Fig. 8 for PSDs that are susceptible to liquefaction does include data that are deemed as not susceptible to liquefaction by existing criteria. But more importantly, they found that PSDs that were known to have liquified all fell into the region denoted by $A < 2/3$ on a normalised entropy diagram. To further confirm this interpretation, Fig. 8 also shows experimental data from soil that did not liquefy. This study suggests that the stability criteria set out by Lőrincz (1986) could, in first instance, predict whether a soil is susceptible to liquefaction based on its normalised entropy coordinates.

4.1 Internal stability rule and liquefaction phenomena applied to RSm

The applicability of the internal stability criterion proposed by Lőrincz (1986) to predict the liquefaction susceptibility of mixtures containing rubber and sand particles (i.e. RSm) is explored here, in a similar manner than that attempted by Barreto et al. (2019). Figure 9 shows 30 PSDs with variable rubber contents on a normalised grading entropy diagram. The data used herein correspond to studies that focused on the determination of the liquefaction potential of RSm. Most of these investigations (Kaneko et al. 2013; Otsubo et al. 2016; Bahadori and Roohollah 2018; Enquan and Qiong 2019; Bernal-Sanchez et al. 2020; Amuthan et al. 2020; Rios et al. 2021) demonstrated that the addition of rubber leads to a lower accumulation of the pore water pressure, when compared to rigid incompressible (i.e. sand) soils. On the other hand, other studies (Promputthangkoon and Hyde 2008; Shariatmadari et al. 2018) evidenced that the addition of rubber can result in a greater liquefaction susceptibility. All the studies herein investigated are characterised for using uniformly graded sands and both sand and RSm samples were prepared under a relative density that ranges between 30% and 75%. The samples were tested under a wide range of confining pressures ranging between 100 kPa and 700 kPa.

Alternatively, this study utilises the normalised entropy coordinates to understand the liquefaction susceptibility of RSm. The methodology used was relatively simple. Experimental data available was assessed in terms of the pore pressure ratio. Specimens in which this ratio reached a value of 1 were considered to have liquefied. Meanwhile the gradation for each specimen which liquefied (or not) was represented by the grading entropy coordinates as shown in Figs. 7 and 8. It can be observed that when doing this, that grading

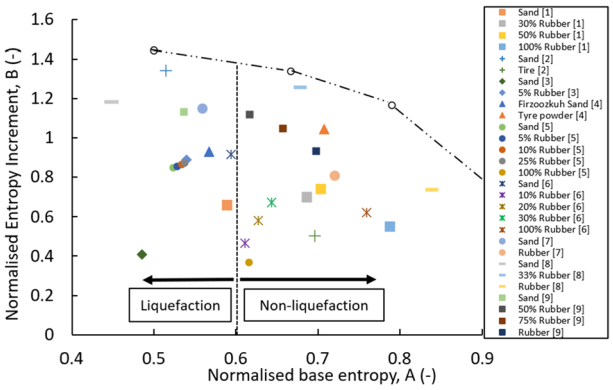

Fig. 9 Stability of RSm based on the literature: [1] = Kaneko et al. 2013; [2] = Otsubo et al. 2016; [3] = Promputthangkoon and Hyde 2008; [4] = Bahadori and Roohollah, 2018; [5] = Shariatmadari et al. 2018; [6] = Bernal-Sanchez et al. 2020, [7] = Enquan and Qiong 2019; [8] = Rios et al. 2021; [9] = Amuthan et al. 2020

entropy coordinates are separated on the normalised entropy diagram in two regions related to the occurrence (or not) of liquefaction.

As shown in Fig. 9, the results point to a variable stability if the criterion proposed by Lőrincz (1986) was followed. All sand only mixtures can be found in the unstable zone (A < 2/3). All these samples are characterised for being better graded than the rubber only samples (i.e. higher B) but having smaller average grain sizes and hence lower A-coordinates. These studies reported that sand soils eventually liquefied due to the accumulation of pore water pressure. So, as occurred in Barreto et al. (2019), the stability criterion proposed by Lőrincz (1986) appears to effectively predict the liquefaction susceptibility of incompressible soils.

In turn, most of the rubber only mixtures from these studies fall into the so-called suffusion zone (as defined in Figs. 7 and 8) due to having a relatively uniform size (i.e. and low B) and a high A value (i.e. A > 2/3). However, according to the previous studies, samples containing 100% rubber did not liquefy and they all exhibited a significant reduction in the liquefaction potential. The latter evidence may partially contradict the criteria established by Lőrincz (1986), but such contradiction may be explained. Rubber particles are well-known for being capable to distort and change its volume under large stresses (Platzer et al. 2018). Moreover, it was found by Fonseca et al. (2019) that rubber particles remain attached to the surrounding particles, 'locking' the possible contact sliding attributable to the high inter-particle friction. Hence, suffusion of rubber particles might not occur in these mixtures because the particles found in the rubber matrix would remain together. So, it may be hypothesised that for soft-rigid mixtures (RSm in particular), the suffusion zone might just be an extension of the stable zone.

Then, two groups can be distinguished for RSm. On one hand, there are the mixtures which experience an increase in the pore water pressure under cyclic loading (Promputthangkoon and Hyde 2008; Shariatmadari et al. 2018). On the other hand, the rest of RSm samples that fall into the initially called unstable zone by Lőrincz (i.e. A < 0.6–0.7) but still did not show an increase in the liquefaction susceptibility according the experimental results. This is the case of 50% and 75% RSm in Amuthan et al. (2020), 10–30% RSm found in Bernal-Sanchez et al. (2020) or the 100% rubber samples studied in Shariatmadari et al. (2018).

As established by Barreto et al. (2019), the PSDs of certain soils can fall on the susceptibility threshold but still be 'stable' when tested under certain experimental conditions. This is because the stability criterion proposed by Lőrincz (1986) only considers particle properties (i.e. PSD) but it does not account for other sample characteristics (e.g. density, particle shape, stiffness, inter-particle friction, and/or mineralogy, etc.) or test conditions (e.g. stress level, stress path, etc.). Of these factors, the relative density is perhaps the most widely recognised parameter influencing liquefaction in soils. Note that the entropy diagram (and the related liquefaction susceptibility criterion proposed here) only provides a quantitative description of the grading. However, this does not imply that the effect of relative density is ignored. For example, the work by Imre et al (2019) highlights that the maximum void ratio of mixtures of sand (e_{max}) may be located at around A = 2/3. This seems to be additional support for the location between stability/susceptibility zones in Figs. 7 and 8. Furthermore, the work by Kabai (1972) also suggested that for many materials the ratio between e_{max} and e_{min} is relatively constant. Therefore, with additional data, the effect of relative density could be further explored/considered. Nevertheless, on the basis of limited data, this study suggests that an alteration of the initially proposed stability zone for mixtures containing compressible (i.e. rubber) particles may be proposed. Consequently, only two zones are suggested in this study: (i) stable and (ii) unstable, as seen in Fig. 9.

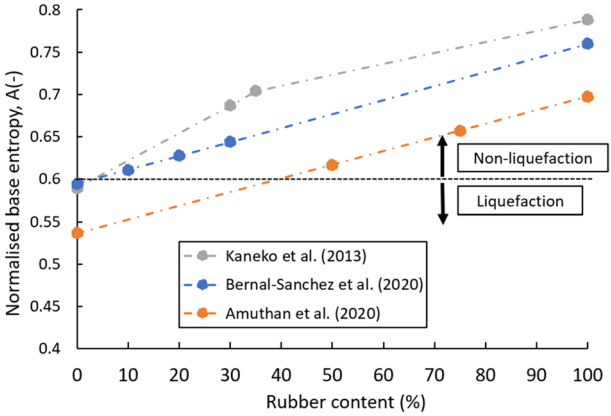

Fig. 10 Normalised base entropy with rubber content of PSDs from Bernal-Sanchez et al. (2020), Amuthan et al. (2020) and Kaneko et al. (2013)

Figure 10 illustrates the normalised based entropy plotted with rubber content for some of the studies previously analysed (Kaneko et al. 2013; Amuthan et al. 2020; Bernal-Sanchez et al. 2020). It is clearly observed that 'A' increases with the rubber content. For the three studies, the addition of rubber points to increasing the normalised base entropy above the 'stability' threshold set by Lőrincz (1986) at A = 2/3. As the 'A' value increases, the number of larger particles carrying a greater proportion of the stress distribution does too (Barreto and Imre 2018). Interestingly, the greater proportion of stress distribution leads inevitably to a reduction in the soil shear stiffness as shown in Fig. 1a. This is due to the low stiffness characteristic of the particulate rubber used in most studies (i.e. G = 1 MPa). The latter finding is also supported by Kaneko et al. (2013) and Amuthan et al. (2020) who showed a significant reduction in the peak shear stress with the rubber content. However, most of the studies coincide in the same finding: adding rubber to sand confers the mixture a nearly elastic, and isotropic, stress–strain behavior which enhances the ability of the sample to deform and recover its size after numerous cycles (Bernal-Sanchez 2020). As a result, undrained RSm exhibit a slower build-up of the pore water pressure with rubber.

Therefore, although the increase in rubber content and the value of 'A' may lead to a reduction in the mixture stiffness, it has an active effect on the soil structure enhancing the stability of the mixture. The latter is demonstrated with the significant reduction in the liquefaction susceptibility demonstrated in existing literature. This may also be explained by the in-filling effects or rubber particles between the voids of rigid sand particles, and to a lesser extent to the supporting effect of rubber particles on strong-force chains formed by sand particles.

Considering the potential use of RSm as a GSI, the results shown in Figs. 9 and 10 suggest that there is a "minimum" value of the normalised based entropy (A) one should aim for in order to minimise the susceptibility of the mixture against liquefaction. It is then established that a mixture should exhibit A > 0.6 to be under the stable zone. As demonstrated in Sect. 3, S_o and A depend on the size ratio between the two particles. Hence, to ascertain whether the mixture reaches the minimum A, the PSD of the two geomaterials (i.e. rubber and sand) needs to be studied at varying rubber proportions using Eqs. 3–4. Although the correlation between A and rubber content is not straightforward (Figs. 9 and 10), mainly due to the variable physical properties of sand and rubber studied, the results

from this study suggest that RSm should contain at least 10–30% rubber to result in a higher internal stability of the mixture.

5 Discussion & conclusions

Given the potential use of RSm as a GSI, this study has explored the effect of PSD on the stiffness and liquefaction susceptibility of RSm using grading entropy coordinates. The relationship between the small-strain shear stiffness of RSm and grading entropy coordinates has been studied using the experimental results from Lee et al. (2010). The stability criterion proposed by Lőrincz (1986) has also inspired a new approach to estimate the liquefaction susceptibility of RSm. It has been explained within the context of the inter-particle force transmission by analysing the relationship between the rubber content and the normalised base entropy (A). The following conclusions can be drawn from this investigation:

- The results from the PSDs obtained by Lee et al. (2010) coincide that the shear stiffness decreases when increasing the rubber content. The latter occurs either when the base entropy (*So*) increases or decreases. However, various trends are observed depending on the size ratio. Lower stiffness degradation is observed on mixtures with either bigger rubber particles ($S_r = 4.7$) or smaller rubber particles ($S_r = 0.5$) as a result of the inter-particle force chains created. The transition between rubber-like and sand-like behaviour and the effect of the size ratio on the stiffness degradation, more evident at 20–50% rubber, has been shown to be affected by *So*.
- By looking at the evolution in the entropy increment (ΔS), it is observed that at similar size ratio ($S_r = 1$) the stiffness decreases with the reduction in ΔS. However, at other size ratios ($S_r = 0.5$, 2, 4.7), the evolution in ΔS follows a different trend, reaching a maximum value before it decreases. The higher value of ΔS may relate to a higher number of inter-particle contacts and hence the evolution of stiffness may be explained in terms of rubber content and size ratio.
- For the studied RSm, stiffness always increases with the stress level. The stiffness has been observed to be dependent on the evolution in the base entropy with rubber content at any size ratio, except for $S_r = 1$. The creation of contour zones has enabled a comparison in the stiffness degradation of RSm with constant size ratio but variable rubber content. At stress levels < 320 kPa, the transition between sand-like and rubber-like behaviour is more pronounced due to the particle-to-particle contacts. As the stress increases (i.e. 320 kPa and 640 kPa), there is minimum change in the stiffness degradation of mixtures with size ratio as a consequence of the high distortion exhibited by rubber particles. At this stress, the macroscopic behaviour is fully controlled by the sand-to-sand contacts.
- The normalised diagram proposed by Lőrincz (1986) has been adopted to study the liquefaction susceptibility of RSm. It has been shown that mixtures containing compressible (i.e. rubber) particles fall, coinciding with the experimental results, in two distinguished zones: i) stable and ii) unstable. This modification of the Lőrincz's original approach has been justified to account for the high inter-particle friction as well as the void filling capacity of rubber particles. Whilst all sand only samples are found in the unstable zone, the opposite occurs with all rubber only mixtures. For the remaining

mixtures, a general trend is that the liquefaction susceptibility reduces with the rubber content.

- It is also evidenced that the addition of rubber leads to increasing the normalised base entropy (A), above the stability threshold proposed by Lőrincz (i.e. $A > 2/3$). The latter phenomenon may be directly related to the number of larger particles carrying a greater proportion of the stress distribution. Although the increase in 'A' is associated with a higher stiffness decay in RSm, it appears to have a beneficial effect on the soil structure enhancing the stability and reducing the liquefaction susceptibility. Therefore, it is recommended in this study that mixtures containing rubber should exhibit $A > 0.6$, normally observed in RSm with more than 10% rubber by mass.

The results obtained from this work demonstrate the grading entropy coordinates are useful and provide alternative means to assess the dependency between stiffness and rubber content, size ratio, stress level, and PSD. This study has also demonstrated that the normalised entropy diagram proposed by Lőrincz can be adopted to understand liquefaction susceptibility of mixtures containing compressible (i.e. rubber) particles.

Further research into the behaviours of the normalised entropy diagram is needed from a micromechanical perspective. Whilst this work has provided a range of PSDs from across the normalised diagram to support the behaviours set out in the stability criteria, a more targeted testing regime should be carried out within each zone. In particular, with the transitions between stable, and unstable regions of the grading entropy-based stability criterion. Also, there are limitations within the grading entropy coordinates because they do not explicitly consider the effects of relative density, particle shape or inherent/induced anisotropy, specimen preparation procedures in laboratory tests, amongst others. Although many of these may be addressed by further research, the approach proposed here seems nevertheless helpful to assess the susceptibility to liquefaction of RSm.

Funding The authors have not disclosed any funding.

Data availability The datasets generated during and/or analysed during the current study are available from the corresponding author on reasonable request.

Declarations

Conflict of interest The authors have not disclosed any competing interests.

References

Amuthan MS, Boominathan A, Banerjee S (2020) Undrained cyclic responses of granulated rubber-sand mixtures. Soils Found 60:871–885

Anastasiadis A, Senetakis K, Pitilakis K (2012) Small-strain shear modulus and damping ratio of sand-rubber and gravel-rubber mixtures. Geotech Geol Eng 30(2):363–382. https://doi.org/10.1007/s10706-011-9473-2

Bahadori H, Farzalizadeh R (2018) Dynamic properties of saturated sands mixed with tyre powders and tyre shreds. Int J Civil Eng 16(4):395–408. https://doi.org/10.1007/s40999-016-0136-9

Barreto D, Imre E (2018) Grading entropy coordinates and shear stiffness in granular materials. IS Atlanta 2018 Paper Abstracts: Particles/crushing II

Barreto D, Leak J, Dimitriadi V, McDougall J (2019) Grading entropy coordinates and criteria for evaluation of liquefaction potential. Earthquake Geotechnical Engineering and Protection and Development of Environment and Constructions 1346–1353

Baziar MH, Dobry R (1995) Residual strength and large-deformation potential of loose silty sands. J Geotech Eng 121:896–906

Bernal-Sanchez J, McDougall J, Barreto D, Miranda M, Marinelli A (2018) Dynamic behaviour of shredded rubber soil mixtures. In: 16th European conference on earthquake engineering, Thessaloniki.

Bernal-Sanchez J, McDougall J, Barreto D, Marinelli A, Dimitriadi V, Anbazhagan P, Miranda M (2019) Experimental assessment of stiffness and damping in rubber-sand mixtures at various strain levels. In: Earthquake goetechnical engineering for protection and development of environment and constructions

Bernal-Sanchez J, McDougall J, Miranda M, Barreto D (2022) Dynamic behaviour of a geotechnical seismic isolation system with rubber-sand mixtures to enhance seismic protection. In: 3rd European conference on earthquake engineering & seismology, Bucharest

Bernal-Sanchez J (2020) Cyclic performance on rubber-soil mixtures to enhance seismic protection. Dissertation, Edinburgh Napier University

European Communities (2006) Implementation of the landfill directive at regional and local level. Office for Official Publications of the European Communities

Edincliler A, Baykal G, Saygılı A (2010) Influence of different processing techniques on the mechanical properties of used tires in embankment construction. Waste Manage 30:1073–1080

Enquan Z, Qiong W (2019) Experimental investigation on shear strength and liquefaction potential of rubber-sand mixtures. Adv Civil Eng. https://doi.org/10.1155/2019/5934961

ETRMA (2015) End of life tyres - Report 2015. https://www.etrma.org/wp-content/uploads/2019/09/elt-report-v9a-final.pdf

Feng S, Vardanega PJ, Ibraim E, Widyatmoko I, Ojum C (2019) Permeability assessment of some granular mixtures.Géotechnique. 69(7): 646–654

Fonseca J, Bernal-Sanchez J, Riaz A, Barreto D, McDougall J, Miranda-Manzanares M, Marinelli A, Dimitriadi V (2019) Particle–scale interactions and energy dissipation mechanisms in sand–rubber mixtures. Géotechnique Letters 9(4):1–6. https://doi.org/10.1680/jgele.18.00221

Fu R, Coop MR, Li XQ (2017) Influence of particle type on the mechanics of sand–rubber mixtures. J Geotech Geoenviron Eng. https://doi.org/10.1061/(asce)gt.1943-5606.0001680

Gobbi S, Reiffsteck P, Avila M, SemblatLenti JFL (2021) Liquefaction triggering in silty sands: effects of non-plastic fines and mixture-packing conditions. Acta Geotechnic. https://doi.org/10.1007/s11440-021-01262-10123456789

Guo T, Prakash S (1999) Liquefaction of silts and silt–clay mixtures. J Geotech Geoenviron Eng 125:706–710

Imre E, Lőrincz J, Trang P, Barreto D, Goudarzy M, Rahemi N, Singh V (2019) A note on seismic induced liquefaction. In: XVII European Conference on Soil Mechanics and Geotechnical Engineering: Conference proceedings. https://doi.org/10.32075/17ECSMGE-2019-0979

Ishihara K (1997) Terzaghi oration: Geotechnical aspects of the 1995 Kobe earthquake. In: Proceedings of 14th International Conference Soil Mechanics & Foundation Engineering 2047–2073

Kabai I (1972) Relationship between the grading curve and the compactibility, PhD thesis, TU of Budapest, Hungary (in Hungarian)

Kaneko T, Orense M, Hyodo P, Yoshimoto N (2013) Seismic response characteristics of saturated sand deposits mixed with tire chips. J Geotech Geoenviron Eng 139(4):633–643. https://doi.org/10.1061/(ASCE)GT.1943-5606.0000752

Kim HK, Santamarina JC (2008) Sand–rubber mixtures (large rubber chips). Can Geotech J 45(10):1457–1466. https://doi.org/10.1139/T08-070

Leak J, Barreto D, Dimitriadi V, Imre E (2021) Revisiting Hardin's parameters for the quantification of particle breakage – a statistical entropy approach. In: The European Physical Journal Conferences. https://doi.org/10.1051/epjconf/202124907001

Leak J, Barreto D, Dimitriadi D, Imre E (2022) Quantifying particle breakage and its evolution using breakage indices and grading entropy coordinates.Geotechnics, 4:1109–1126. https://doi.org/10.3390/geotechnics2040052

Lee JS, Dodds J, Santamarina JC (2007) Behavior of rigid-soft particle mixtures. J Mater Civ Eng 19(2):179–184. https://doi.org/10.1061/(ASCE)0899-1561(2007)19:2(179)
Lee C, Truong QH, Lee W, Lee JS (2010) Characteristics of rubber-sand particle mixtures according to size ratio. J Mater Civ Eng 22(4):323–331. https://doi.org/10.1061/(ASCE)MT.1943-5533.0000027
Lőrincz J, Imre E, Gálos M, Trang QP, Rajkai K, Fityus S, Telekes G (2005) Grading entropy variation due to soil crushing. Int J Geomech 5(4):311–319
Lőrincz J (1986) Grading entropy of soils. Dissertation, Technical University of Budapest (in Hung)
Mahdavisefat E, Salehzadeh H, Heshmati AA (2017) Full-scale experimental study on screening effectiveness of SRM-Filled Trench Barriers. Géotechnique. https://doi.org/10.1680/jgeot.17.P.007
Masad E, Taha R, Ho C, Papagiannakis T (1996) Engineering properties of tire/soil mixtures as a lightweight fill material. Geotech Test J 19(3):297–304. https://doi.org/10.1520/GTJ10355J
Mashiri MS, Vinod JS, Sheikh MN (2016) Liquefaction potential and dynamic properties of sand-tyre chip (stch) mixtures. Geotech Test J. https://doi.org/10.1520/GTJ20150031
O'Kelly BC, Nogal M (2020) Determination of soil permeability coefficient following an updated grading entropy approach. Geotech Research 7(1):58–70. https://doi.org/10.1680/jgere.19.00036
Okashi Y (1970) Effects of sand compaction on liquefaction during Tokachioki earthquake. Soils Found 10(2):112–128
Oquendo-Patiño WF, Estrada N (2022) Finding the grain size distribution that produces the densest arrangement in frictional sphere packings: Revisiting and rediscovering the century-old Fuller and Thompson distribution. Phys Rev. https://doi.org/10.1103/PhysRevE.105.064901
Otsubo M, Towhata I, Hayashida T, Liu B, Goto S (2016) Shaking table tests on liquefaction mitigation of embedded lifelines by backfilling with recycled materials. Soils Found 56(3):365–378
Perlea VG (2000) Liquefaction of cohesive soils. Soil Dyn Liquefact 107:58–76
Platzer A, Rouhanifar S, Richard P, Cazacliu B, Ibraim E (2018) Sand–rubber mixtures undergoing isotropic loading: derivation and experimental probing of a physical model. Gran Matt 20(4):1–10. https://doi.org/10.1007/s10035-018-0853-7
Promputthangkoon P, Hyde AFL (2008) Compressibility and liquefaction potential of rubber composite soils. International workshop on scrap tire derived geomaterials – opportunities and challenges 161–170
Rees S (2010) Effects of fines on the undrained behaviour of christchurch sandy soils. Dissertation, University of Canterbury, Christchurch, New Zealand
Rios S, Kowalska M, Viana da Fonseca A (2021) Cyclic and dynamic behavior of sand–rubber and clay–rubber mixtures. Geotech Geol Eng 39:3449–3467
Senetakis K, Anastasiadis A, Pitilakis K (2012) Dynamic properties of dry sand/rubber (SRM) and gravel/rubber (GRM) mixtures in a wide range of shearing strain amplitudes. Soil Dyn Earthq Eng 33(1):38–53. https://doi.org/10.1016/j.soildyn.2011.10.003
Shariatmadari N, Karimpour-Fard M, Shargh A (2018) Undrained monotonic and cyclic behavior of sand-ground rubber mixtures. Earthq Eng Eng Vib 17(3):541–553. https://doi.org/10.1007/s11803-018-0461-x
Sheikh MN, Mashiri MS, Vinod JS, Tsang HH (2012) Shear and compressibility behaviours of sand-tyre crumb mixtures. J Mater Civil Eng. https://doi.org/10.1061/(ASCE)MT.1943-5533.0000696
Thevanayagam S (1998) Effects of fines and confining stress on undrained shear strength of silty sands. J Geotech Geoenviron Eng 124(6):479–491
Tokimatsu K, Yoshimi Y (1983) Empirical correlation of soil liquefaction based on spt n-value and fines content. Soils Found 23:56–74
Tsai PH, Lee DH, Kung GTC, Hsu CH (2019) Effect of content and plasticity of fines on liquefaction behaviour of soils. Q J Eng GeolHydrogeol 43:95–106. https://doi.org/10.1144/1470-9236/08-019
Tsang HH, Pitilakis K (2019) Mechanism of geotechnical seismic isolation system: analytical modelling. Soil Dyn Earthq Eng 122:171–184
Tsang HH, Lo SH, Xu X, Sheikh MN (2012) Seismic isolation for low-to-medium rise buildings using granulated rubber-soil mixtures: numerical study. Earthquake Eng Struct Dynam 41(14):2009–2024. https://doi.org/10.1002/eqe.2171
Tsang HH, Tran DP, Hung WY, Pitilakis K, Gad EF (2021) Performance of geotechnical seismic isolation system using rubber-soil mixtures in centrifuge testing. Earthquake Eng Struct Dynam 50(5):1271–1289
Tsang HH (2009) Geotechnical seismic isolation. Earthquake Engineering: New Research 55–87
Wichtmann T, Triantafyllidis T (2009) Influence of the grain-size distribution curve of Quartz sand on the small strain Shear modulus Gmax. J Geotech Geoenviron Eng 135(10):1404–1418. https://doi.org/10.1061/(ASCE)GT.1943-5606.0000096
Xiong W, Li Y (2013) Seismic isolation using granulated tire-soil mixtures for less-developed regions: experimental validation. Earthquake Eng Struct Dyn 42(14): 2187–2193. https://doi.org/10.1002/eqe.2315

Youwai S, Bergado DT (2003) Strength and deformation characteristics of shredded rubber tire - sand mixtures. Can Geotech J 40(2):254–264. https://doi.org/10.1139/t02-104

Zornberg JG, Cabral AR, Viratjandr C (2004) Behaviour of tire shred-sand mixtures. Can Geotech J 41(2):227–241. https://doi.org/10.1139/t03-086.D